Improved Propagation Modeling in Ultra-Wideband Indoor Communication Systems Utilizing Vector Fitting Technique of the Dielectric Properties of Building Materials

Konstantinos P. Prokopidis*, Dimitrios C. Zografopoulos†, Christos Kalialakis‡, and Apostolos Georgiadis§

*Department of Electrical and Computer Engineering, Aristotle University of Thessaloniki, Thessaloniki GR-54124, Greece Email: kprokopi@ee.auth.gr

†Consiglio Nazionale delle Ricerche, Istituto per la Microelettronica e Microsistemi (CNR-IMM), Roma 00133, Italy Email: dimitrios.zografopoulos@artov.imm.cnr.it

‡Centre Tecnologic de Telecomunicacions de Catalunya-CTTC, Castelldefels 08860, Barcelona, Spain Email: christos.kalialakis@cttc.es

§Institute of Sensors, Signals and Systems, School of Engineering and Physical Sciences, Heriot-Watt University, Edinburgh, Scotland, UK Email: apostolos.georgiadis@ieee.org

***Abstract*—This paper demonstrates the application of the Finite-Difference Time-Domain method for dispersive media to indoor ultra-wideband channel modeling. A new description of the frequency dispersion of building materials, based on a partial-fraction approach, is proposed, utilizing experimentally measured data on complex permittivity values reported in the literature. The analytical dispersion model for a series of building materials is estimated through the Vector Fitting technique and the through-the-wall penetration is calculated for indicative cases. Finally, a small two-dimensional office environment is studied and several channel characteristics are calculated demonstrating the flexibility and robustness of the proposed formulation in communication modeling. The proposed FDTD implementation covers all the bandwidth in a single run instead of running simulations for every frequency or subband.**

I. Introduction

Following the increasing interest in ultra-wideband (UWB) systems [1], [2] during the last years, the need for radio network planning tools that aid operators to design and optimize their wireless infrastructure is rising. In order to increase the reliability of these tools and to successful implement such systems, assiduous study of the propagation channel is necessary.

Currently used techniques make use of empirical or semi-empirical models due to their quick implementation and short running time. However, these models suffer from a lack of precision in complex environments such as urban and indoor scenarios, where the various obstacles should be more accurately modeled. It is thus necessary to make use of deterministic models based on physical laws that try to compute the reflection, diffraction, transmission and scattering on obstacles.

Ray-tracing [3] and geometric-like models have been proposed to this end. They have shown to be very efficient, except in severe environments, where a large number of multipath reflections need to be computed, and where the diffraction phenomena, even with the Uniform Theory of Diffraction (UTD), are difficult to simulate.

Another well known approach to compute radio wave propagation is the Finite-Difference Time-Domain (FDTD) method [4], which solves directly Maxwell's equations on the nodes of a discrete grid. This method is very appealing, since it rigorously takes into account wave-matter interaction. In several works [5]–[13], FDTD formulations are exploited in 2- and 3-D implementations for the study of propagation mechanisms for indoor or between nearby buildings communications. In all the aforementioned works the material modeling is restricted either to non-dispersive media or lossy materials with a static conductivity term.

In this work, we exploit the time-domain nature of the FDTD technique by also taking into account the frequency dependent material properties. Instead of running individual simulations for every single frequency or subband of interest, all relevant information is obtained using a wide frequency content excitation pulse in a single run with the aid of the Fourier transform. This property renders the FDTD method an indispensable tool for the study of wideband propagation channels. Especially, in UWB systems where the bandwidth is greater than 500 MHz and sometimes several GHz, the dielectric permittivity and the losses of building materials vary significantly in such large frequency ranges. Furthermore, the proposed formulation avoids the division of the frequency band of interest into subbands as presented in [8].

Although the main disadvantage of the FDTD method to solve electrically large problems is the excessive computational requirements, advances in processing capabilities (multicore CPU, graphical processing units (GPU)) and par-

TABLE I
PF FITTED PARAMETERS OF SOLID CONCRETE BASED ON MEASUREMENTS REPORTED IN [17].

Parameter	Value
ϵ_∞	6.3
a_1	-3.0268×10^{10} rad/sec
c_1	-1.4263×10^{10} rad/sec
a_2	-1.5923×10^{10} rad/sec
c_2	4.6218×10^{10} rad/sec

TABLE II
PF FITTED PARAMETERS OF PLYWOOD BASED ON MEASUREMENTS REPORTED IN [17].

Parameter	Value
ϵ_∞	2.1
a_1	$(-0.00789 \pm 0.5010j) \times 10^{10}$ rad/sec
c_1	$(0.4138 \mp 3.0340j) \times 10^{8}$ rad/sec
a_2	$(-0.5619 \pm 1.4077j) \times 10^{10}$ rad/sec
c_2	$(8.3735 \mp 3.7212j) \times 10^{8}$ rad/sec

allel computing are making their application to the indoor propagation problem tractable [14], [15].

In the present work the permittivity of several building materials is fitted to a partial-fraction (PF) function using the Vector Fitting technique [16]. VF is a robust method extensively used from high-voltage power systems to microwave systems and high-speed electronics and produces guaranteed stable poles that are real or come in complex conjugate pairs. In Section II, the fitted functions are fed into the developed dispersive FDTD technique based on PF terms and applied in 1-D and 2-D problems (Section III). The investigated examples of Section IV demonstrate that the proposed numerical framework is an effective tool in the study and design of indoor communication systems, restricted only by the power of available computational resources. Finally, in Section V, the conclusions are drawn.

II. MODELING OF BUILDING MATERIALS WITH PF MODELS

Most materials in nature exhibit frequency dependent electromagnetic characteristics, a property which is described by the term *frequency dispersion* [18]. Various dispersion functions have been extensively used to describe the variation of media complex permittivity, including Debye, Drude, Lorentz, Cole-Cole, and Davidson-Cole models. Typically, the parameters of the dispersion functions are estimated by a fitting process of experimentally acquired data during material characterization. In recent years, additional dielectric functions, e.g. complex-conjugate pole-residue pairs [19], Drude-critical points [20], and the modified Lorentz model [21], have been proposed for the accurate representation of material dispersion, such as in the case of metals, semiconductors, and graphene, in the optical/IR and THz frequencies. It can be proved that all of the aforementioned models can be incorporated in a generalized form based on partial fractions (PF) [22], [23]. In

TABLE III
PF FITTED PARAMETERS OF HOLLOW CONCRETE BASED ON MEASUREMENTS REPORTED IN [17].

Parameter	Value
ϵ_∞	2.8
a_1	$(-0.78607 \pm 0.5706j) \times 10^{10}$ rad/sec
c_1	$(1.9365 \mp 0.1166j) \times 10^{10}$ rad/sec
a_2	$(-0.57466 \pm 1.0503j) \times 10^{10}$ rad/sec
c_2	$(-0.6805 \pm 1.3468j) \times 10^{10}$ rad/sec
a_3	$(-0.4085 \pm 1.2842j) \times 10^{10}$ rad/sec
c_3	$(-0.3116 \mp 0.62139j) \times 10^{10}$ rad/sec

TABLE IV
PF FITTED PARAMETERS OF BRICK BASED ON MEASUREMENTS REPORTED IN [24].

Parameter	Value
ϵ_∞	2.5
a_1	-0.02531×10^{10} rad/sec
c_1	0.02217×10^{10} rad/sec
a_2	-2.8311×10^{10} rad/sec
c_2	2.457694×10^{10} rad/sec
a_3	$(-0.03106 \pm 2.2926j) \times 10^{10}$ rad/sec
c_3	$(0.004512 \mp 0.02679j) \times 10^{10}$ rad/sec

the PF model, the relative permittivity is described via

$$\varepsilon(\omega) = \varepsilon_\infty + \sum_{p=1}^{M} \chi_p(\omega), \tag{1}$$

with the susceptibility function defined as

$$\chi_p(\omega) = \begin{cases} \frac{c_p}{j\omega - a_p}, & \text{if } a_p \text{ is real} \\ \frac{c_p}{j\omega - a_p} + \frac{c_p^*}{j\omega - a_p^*}, & \text{if } a_p \text{ is complex} \end{cases} \tag{2}$$

where ε_∞ is the relative permittivity at infinite frequency, c_p and a_p are the poles and residues, respectively, and $*$ denotes the complex conjugate. Although PF models have been applied to model metals in optical/IR spectrum, such models have not been applied yet for the frequency description of the permittivity of media such as building materials in the microwave bands.

In the present work we describe the dielectric properties of building materials encountered in wireless communication systems using the PF formulation and estimate the parameters of the model through the VF technique [16]. VF is a robust numerical method for rational approximation in the frequency domain using poles and residues, which is widely used to calculate a reduced-order passive macromodel for the characterization of terminal frequency responses. The resulting rational expression has stable poles, real or complex conjugate pairs, which are compatible with the PF formulation of (1). We use tabulated measured data for solid concrete, plywood, hollow concrete [17] and brick [24] and the parameters yielded by the VF technique are shown in Tables I-IV.

In Fig. 1 the real and the imaginary parts of dielectric permittivities of the fitted functions are shown against the measurement data for each material under consideration. It

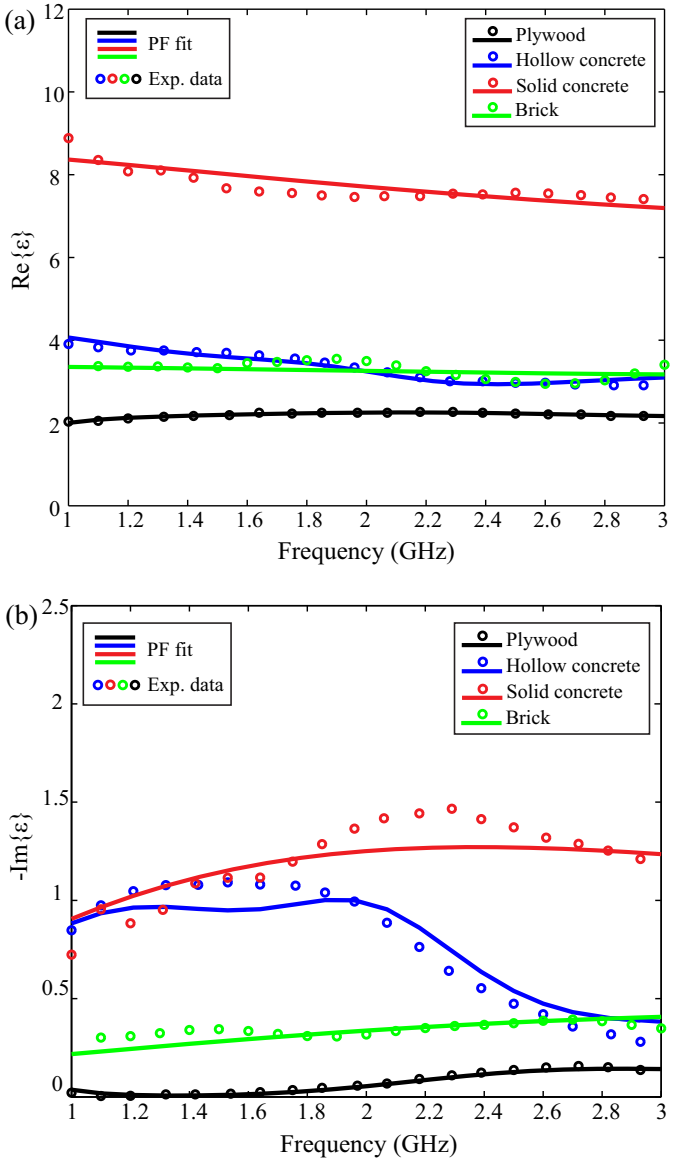

Fig. 1. (a) Real and (b) imaginary part of the dielectric permittivity of the fitted models and the measurement data for plywood, hollow concrete, solid concrete and brick.

is noted that the fitted models can also be used in nondestructive evaluation, grounding penetrating radars [25] and other engineering applications. Additionally, the proposed PF modeling of materials can be also exploited in other time-domain methods in computational electromagnetics e.g. finite-integration technique.

III. FDTD Formulation with PF Dispersive Models

We start the derivation of the FDTD formulation used in the following simulations, from the Ampére-Maxwell equation in the frequency domain

$$j\omega\varepsilon_0\,\varepsilon(\omega)\,\boldsymbol{E}(\omega) = \nabla\times\boldsymbol{H}(\omega), \tag{3}$$

where $\varepsilon(\omega)$ is the frequency-dispersive relative permittivity of the medium, which is assumed to follow (2).

The term $j\omega\varepsilon_0\varepsilon(\omega)\boldsymbol{E}(\omega)$ for the case of complex a_p in (2) can be written as

$$j\omega\varepsilon_0\varepsilon_o(\omega)\boldsymbol{E}(\omega) = j\omega\varepsilon_0\varepsilon_\infty\boldsymbol{E}(\omega) + \sum_p \boldsymbol{J}_p(\omega) + \sum_p \boldsymbol{J}'_p(\omega), \tag{4}$$

by introducing the additional variables $\boldsymbol{J}_p$ and $\boldsymbol{J}'_p$ defined as

$$\boldsymbol{J}_p(\omega) = j\omega\varepsilon_0\frac{c_p}{j\omega - a_p}\,\boldsymbol{E}(\omega), \tag{5}$$

$$\boldsymbol{J}'_p(\omega) = j\omega\varepsilon_0\frac{c^*_p}{j\omega - a^*_p}\,\boldsymbol{E}(\omega). \tag{6}$$

Equations (5)-(6) are transformed into the time domain as

$$\frac{d\boldsymbol{J}_p}{dt} - a_p\boldsymbol{J}_p = \varepsilon_0 c_p\frac{d\boldsymbol{E}}{dt}, \tag{7}$$

$$\frac{d\boldsymbol{J}'_p}{dt} - a^*_p\boldsymbol{J}'_p = \varepsilon_0 c^*_p\frac{d\boldsymbol{E}}{dt}. \tag{8}$$

Given that in the time domain the electric field component $\boldsymbol{E}$ is a real quantity, i.e. $d\boldsymbol{E}^*/dt = d\boldsymbol{E}/dt$, it can be concluded that $\boldsymbol{J}'_p = \boldsymbol{J}^*_p$. Moreover, since $z + z^* = 2\Re\{z\}$ with $\Re\{\cdot\}$ denoting the real part of a complex value, (4) in the time domain becomes

$$\varepsilon_0\varepsilon_\infty\frac{d\boldsymbol{E}}{dt} + \sum_p\left(\boldsymbol{J}_p + \boldsymbol{J}'_p\right) = \varepsilon_0\varepsilon_\infty\frac{d\boldsymbol{E}}{dt} + \sum_p 2\,\Re\{\boldsymbol{J}_p\}. \tag{9}$$

In case a_p is a real pole, (5) holds and one obtains

$$\varepsilon_0\varepsilon_\infty\frac{d\boldsymbol{E}}{dt} + \sum_p\left(\boldsymbol{J}_p + \boldsymbol{J}'_p\right) = \varepsilon_0\varepsilon_\infty\frac{d\boldsymbol{E}}{dt} + \sum_p \boldsymbol{J}_p, \tag{10}$$

since $\boldsymbol{J}_p$ is in this case a real quantity and $\boldsymbol{J}'_p$ is zero. In both cases, only $\boldsymbol{J}_p$ is needed to be updated and stored in memory.

Taking into account (4), (3) in the time domain is written as

$$\nabla\times\boldsymbol{H} = \varepsilon_0\varepsilon_\infty\frac{d\boldsymbol{E}}{dt} + \sum_p \xi_p\Re\{\boldsymbol{J}_p\}, \tag{11}$$

where both cases described by (9) and (10) are unified via the addition of the extra parameter ξ_p, defined as

$$\xi_p = \begin{cases} 1, & \text{if } a_p \text{ is real,} \\ 2, & \text{if } a_p \text{ is complex} \end{cases}. \tag{12}$$

Equation (5) is also transformed into the time domain

$$\frac{d\boldsymbol{J}_p}{dt} - a_p\boldsymbol{J}_p = \varepsilon_0 c_p\frac{d\boldsymbol{E}}{dt}, \tag{13}$$

and after discretization at time step $n+1/2$ we get

$$\frac{\delta_t\boldsymbol{J}_p^{n+1/2}}{\Delta t} - a_p\mu_t\boldsymbol{J}_p^{n+1/2} = \varepsilon_0 c_p\frac{\delta_t\boldsymbol{E}^{n+1/2}}{\Delta t}, \tag{14}$$

where δ_t and μ_t are the central difference and average operators over Δt, respectively, defined as $\delta_t F^n = F^{n+1/2} - F^{n-1/2}$, $\mu_t F^n = 0.5(F^{n+1/2} + F^{n-1/2})$. Finally, we obtain the following update equation

$$\boldsymbol{J}_p^{n+1} = d_{1p}\boldsymbol{J}_p^n + d_{2p}\boldsymbol{E}^{n+1} + d_{3p}\boldsymbol{E}^n, \tag{15}$$

with

$$d_{1p} = \frac{1 + a_p \Delta t/2}{1 - a_p \Delta t/2},\ d_{2p} = \frac{\varepsilon_0 c_p}{1 - a_p \Delta t/2}\, d_{3p} = -d_{2p}. \quad (16)$$

Similarly, (11) is discetized at time step $n + 1/2$

$$\nabla \times \boldsymbol{H}^{n+1/2} = \varepsilon_0 \varepsilon_\infty \frac{\delta_t \boldsymbol{E}^{n+1/2}}{\Delta t} + \sum_p \xi_p \Re\{\mu_t \boldsymbol{J}_p^{n+1/2}\}. \quad (17)$$

Using (15) in (17) the update equation of the $\boldsymbol{E}$ is yielded

$$\boldsymbol{E}^{n+1} = C_1 \Big(C_2 \boldsymbol{E}^n - \frac{1}{2} \sum_p \xi_p \Re\{(1 + d_{1p}) \boldsymbol{J}_p^n\} + \nabla \times \boldsymbol{H}^{n+1/2} \Big), \quad (18)$$

where

$$C_1 = \frac{\Delta t}{\varepsilon_0 \varepsilon_\infty + 0.5 \Delta t \sum_p \xi_p \Re\{d_{2p}\}}, \quad (19a)$$

$$C_2 = \varepsilon_0 \varepsilon_\infty / \Delta t - 0.5 \sum_p \xi_p \Re\{d_{3p}\}. \quad (19b)$$

The Faraday-Maxwell equation is discretized as in the standard FDTD scheme [4].

The most common criticism of using FDTD method in propagation modeling is the overwhelming CPU and memory requirements. In fact, the proposed technique demand M complex variables, where M is the number of PF terms in (1) for storing each component of $\boldsymbol{J}_p$ per FDTD cell, i.e. $48M$ additional bytes over the standard FDTD method for the 3D case when double precision is used. The modeling of a moderate office environment of dimensions $20\text{m} \times 20\text{m}$ in 2D using the proposed method with 3 PF terms and assuming FDTD cell size $\lambda_{\min}/20$ with maximum frequency of interest 3 GHz demands approximately 1 GB of memory. Finally, the updating of each component of $\boldsymbol{J}_p$ and $\boldsymbol{E}$ involves $4M$ additional complex multiplications per FDTD cell. It is noted that the emerging technologies of clustering computing [14] are making the study of indoor propagation problem using FDTD approaches tractable.

The present method goes beyond current capabilities of time domain commercial simulators. The results given in the following section were produced with an in-house FDTD code written in MATLAB which has also been extended to more complicated dispersive/anisotropic materials [26].

IV. Numerical Results

A. Through-the-Wall Penetration Loss

As a benchmark problem, we study the penetration loss through walls of different material and thickness using the proposed numerical formulation in comparison to analytical solutions [27]. We consider 10-cm and 5-cm walls made of brick, plywood and solid concrete. A plane wave impinges perpendicularly on the wall and the material dispersion is described via the PF model as explained in Section 2 with parameters shown in Tables I, II, and IV. The FDTD code ran with $\Delta = 1$ mm and $\Delta t = 0.3\Delta z/c_0$, where c_0 is the velocity of light in vacuum. The computational domain was backed with a 12-cell Convolution Perfectly Matched Layer (CPML) [28] and the excitation source was a modulated Gaussian pulse with frequency content in the region $1 - 3$ GHz. In Fig. 2 the penetration loss is calculated, demonstrating acceptable

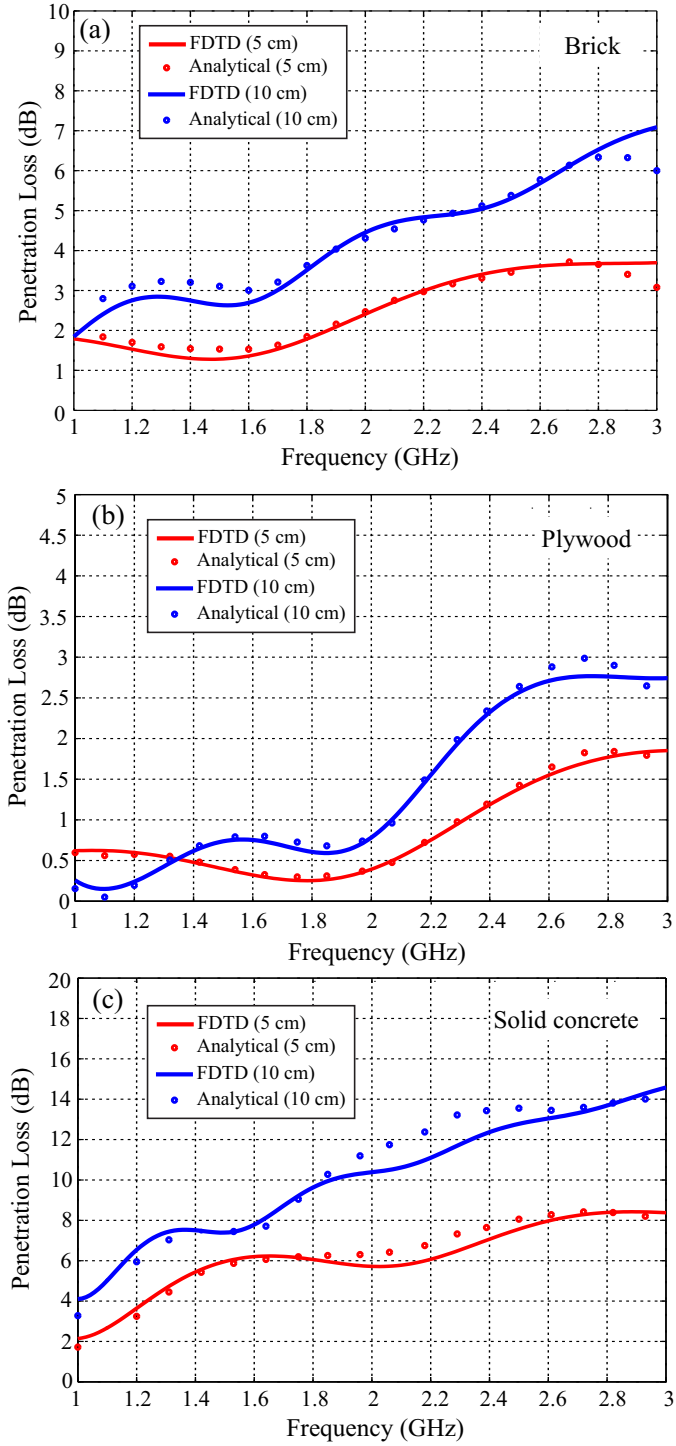

Fig. 2. Penetration loss through a (a) brick, (b) plywood and (c) solid concrete wall of thickness 5 cm and 10 cm. FDTD results using the fitted PF dispersion model are compared to the analytical solution calculated for the experimentally measured permittivity values.

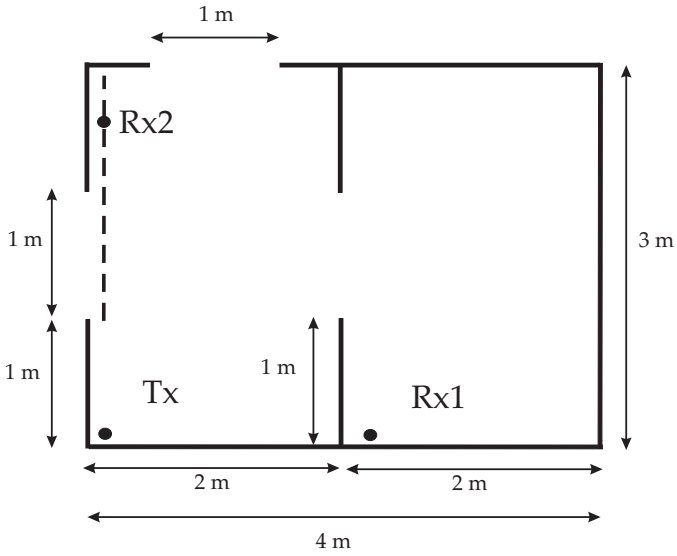

Fig. 3. Floor plan of the two-dimensional office under study. The transmitter (Tx) and the receivers' (Rx1 and Rx2) locations are shown. The dashed line indicates the path along which power loss is calculated in Fig. 6.

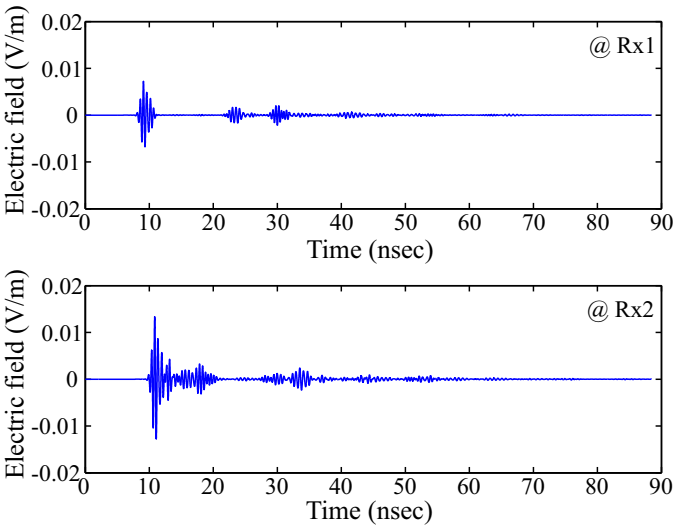

Fig. 4. Electric field as a function of time at Rx1 and Rx2.

agreement between the FDTD and the reference solution. The divergence between the numerical solution and the analytical one is owing to the quality of the fitting since the numerical dispersion of the FDTD method is negligible with the chosen space step Δ.

B. UWB Channel Characterization of Two-dimensional Environment

The floor plan of a two-dimensional office environment selected as a case-study is shown in Fig. 3. The walls are 5 cm thick and made of solid concrete, which is modeled as a dispersive material with parameters as in Table I. Transverse magnetic (TM) polarized field is considered with FDTD cells of $\Delta x = \Delta y = 5$ mm and time step was chosen 3.538×10^{-12} sec. The stability criterion of the presented FDTD method

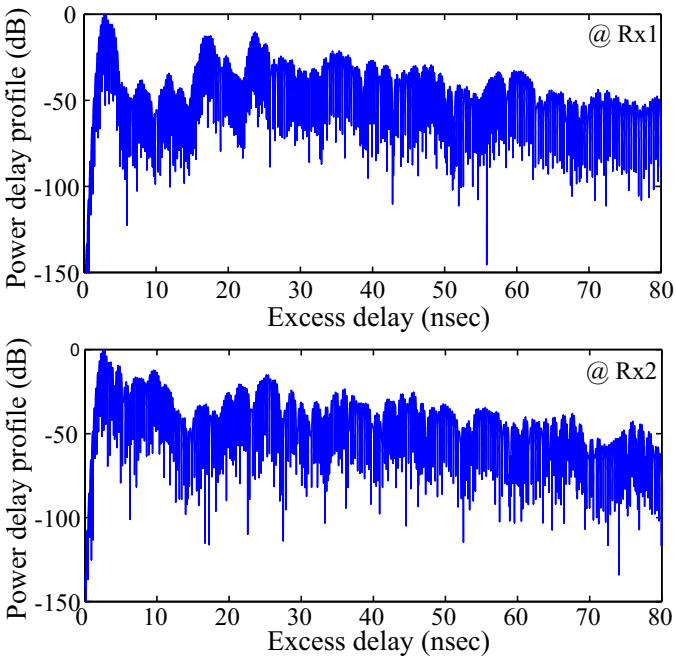

Fig. 5. Power Delay Profile at Rx1 and Rx2.

can be extracted by an analogous manner of [29]. The FDTD code ran for 25000 time steps in a computational domain of 836×636 cells. A single field component E_z is used for the excitation with frequency content in the region $1 - 3$ GHz. The FDTD grid resolution corresponds to $\lambda_{\min}/20$, while the computational domain is terminated by a 8-cell CPML [28]. In Fig. 4, the electric field is shown at the receivers' locations. It is observed that the amplitude of the direct wave in Rx1 is lower than the corresponding in Rx2 because Rx1 is behind the wall. The profile of the recorded time-domain signals in Fig. 4 reveals various late-time pulses arriving at the receivers, owing to reflections at the room's walls. In Fig. 5 the power delay profiles, normalized over the maximum received field, are shown for Rx1 and Rx2.

In Fig. 6 the path loss is calculated for the path depicted in Fig. 3 for two different frequencies around 2.42 GHz and 2.82 GHz. The path loss exponent is also calculated obtaining, as expected, values lower than that of an isotropic antenna, owing to the positioning of the transmitter at the corner of the room, where back-reflections enhance the transmittance towards the path where power loss is calculated. It is stressed that the calculation for both frequencies was done using Discrete Fourier Transform (DFT) of the stored electric field in the locations of the path after the FDTD simulation. One of the strengths of the proposed time-domain formulation is the ability to extract results in the whole frequency of interest with a single simulation. In Fig. 6 the path loss exponent is also depicted.

V. Conclusion

Wideband characterization of the building material permittivity is obtained through fitting processes based on the vector

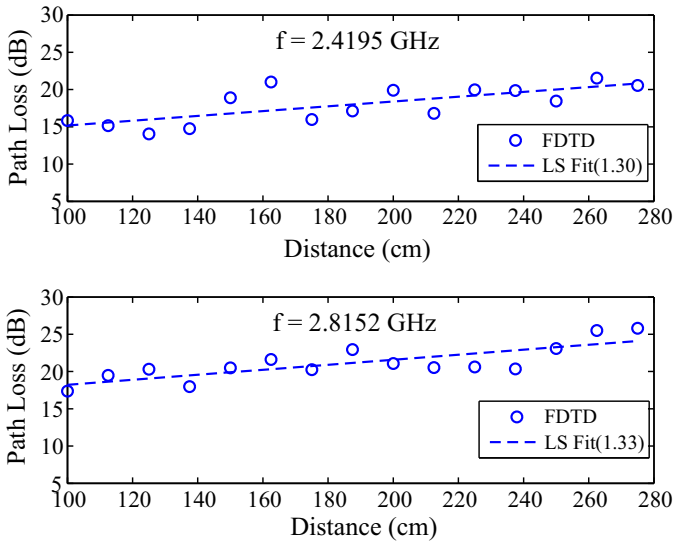

Fig. 6. Path loss calculated from 1 to 2.7 m away from the transmitter, as indicated in Fig. 3. The least square (LS) fitted lines and the values of path loss exponent (in parentheses) are also shown

fitting technique. Full-wave time-domain numerical analysis of indoor propagation channels by rigorously incorporating material dispersion is presented. The proposed framework can be an alternative to empirical models and with the advances in processing computer power can lead to accurate propagation studies of UWB systems.

ACKNOWLEDGMENT

The work of Christos Kalialakis and Apostolos Georgiadis has been supported by European Union Horizon 2020 research and innovation programme under the Marie Skłodowska-Curie grant agreement No 654734.

REFERENCES

[1] J. H. Reed, Ed., *An Introduction to Ultra Wideband Communication Systems*. Prentice Hall, 2005.

[2] B. Allen, M. Dohler, E. Okon, W. Malik, A. Brown, and D. Edwards, *Ultra Wideband Antennas and Propagation for Communications, Radar and Imaging*. Wiley, 2006.

[3] C.-F. Yang, B.-C. Wu, and C.-J. Ko, "A ray-tracing method for modeling indoor wave propagation and penetration," *IEEE Trans. Antennas Propagat.*, vol. 46, no. 6, pp. 907–919, Jun 1998.

[4] A. Taflove and S. C. Hagness, *Computational Electrodynamics: The Finite-Difference Time-Domain Method.* Norwood, MA: 3rd ed., Artech House, 2005.

[5] J. W. Schuster and R. J. Luebbers, "Comparison of GTD and FDTD predictions for UHF radio wave propagation in a simple outdoor urban environment," in *Antennas and Propagation Society International Symposium*, vol. 3, Montreal, Canada, July 13-18, 1997, pp. 2022–2025.

[6] Z. Yun, M. F. Iskander, and Z. Zhang, "Complex-wall effect on propagation characteristics and MIMO capacities for an indoor wireless communication environment," *IEEE Trans. Antennas Propagat.*, vol. 52, no. 4, pp. 914–922, April 2004.

[7] T. T. Zygiridis, E. P. Kosmidou, K. P. Prokopidis, N. V. Kantartzis, C. S. Antonopoulos, K. I. Petras, and T. D. Tsiboukis, "Numerical modeling of an indoor wireless environment for the performance evaluation of wlan systems," *IEEE Trans. Magn.*, vol. 42, no. 4, pp. 839–842, April 2006.

[8] Y. Zhao, Y. Hao, and C. Parini, "FDTD characterization of UWB indoor radio channel including frequency dependent antenna directivities," *IEEE Antennas Wireless Propag. Lett.*, vol. 6, pp. 191–194, 2007.

[9] A. Alighanbari and C. D. Sarris, "Parallel time-domain full-wave analysis and system-level modeling of ultrawideband indoor communication systems," *IEEE Trans. Antennas Propagat.*, vol. 57, no. 1, pp. 231–240, Jan 2009.

[10] A. C. M. Austin, M. J. Neve, G. B. Rowe, and R. J. Pirkl, "Modeling the effects of nearby buildings on inter-floor radio-wave propagation," *IEEE Trans. Antennas Propagat.*, vol. 57, no. 7, pp. 2155–2161, July 2009.

[11] A. C. M. Austin, M. J. Neve, and G. B. Rowe, "Modeling propagation in multifloor buildings using the FDTD method," *IEEE Trans. Antennas Propagat.*, vol. 59, no. 11, pp. 4239–4246, Nov 2011.

[12] A. C. M. Austin and C. D. Sarris, "Ultra-wideband interference modelling for indoor wireless channels using the FDTD method," in *Proceedings of the 2012 IEEE International Symposium on Antennas and Propagation*, Chicago, Illinois, USA, July 8-14, 2012, pp. 1–2.

[13] A. C. M. Austin, "Performance estimation for indoor wireless systems using FDTD method," *Electron. Lett.*, vol. 51, no. 17, pp. 1376–1378, 2015.

[14] W. Yu, R. Mittra, T. Su, Y. Liu, and X. Yang, *Parallel Finite-Difference Time-Domain Method*. Norwood, MA: Artech House, 2006.

[15] M. L. Stowell, B. J. Fasenfest, and D. A. White, "Investigation of radar propagation in buildings: A 10-billion element cartesian-mesh FETD simulation," *IEEE Trans. Antennas Propagat.*, vol. 56, no. 8, pp. 2241–2250, Aug 2008.

[16] B. Gustavsen and A. Semlyen, "Rational approximation of frequency domain responses by vector fitting," *IEEE Trans. Power Del.*, vol. 14, no. 3, pp. 1052–1061, July 1999.

[17] C. Thajudeen, A. Hoorfar, F. Ahmad, and T. Dogaru, "Measured complex permittivity of walls with different hydration levels and the effect on power estimation of TWRI target returns," *Prog. Electromag. Res. B*, vol. 30, pp. 177–199, 2011.

[18] G. Raju, *Dielectrics in Electric Fields*. New York: Marcel Dekker, 2003.

[19] M. Han, R. Dutton, and S. Fan, "Model dispersive media in finite-difference time-domain method with complex-conjugate pole-residue pairs," *IEEE Microw. Wireless Compon. Lett.*, vol. 16, no. 3, pp. 119–121, Mar. 2006.

[20] A. Vial and T. Laroche, "Description of dispersion of metals by means of the critical points model and application to the study of resonant structures using the FDTD method," *J. Phys. D: Appl. Phys.*, vol. 40, pp. 7152–7158, 2007.

[21] A. Deinega and S. John, "Effective optical response of silicon to sunlight in the finite-difference time-domain method," *Opt. Lett.*, vol. 37, no. 1, pp. 112–114, Jan. 2012.

[22] L. Han, D. Zhou, K. Li, X. Li, and W.-P. Huang, "A rational-fraction dispersion model for efficient simulation of dispersive material in FDTD method," *J. Lightwave Technol.*, vol. 30, no. 13, pp. 2216–2225, July 2012.

[23] K. Michalski, "On the low-order partial-fraction fitting of dielectric functions at optical wavelengths," *IEEE Trans. Antennas Propagat.*, vol. 61, no. 12, pp. 6128–6135, Dec. 2013.

[24] R. Kubacki, "New attempt to building materials permittivity measurements." in *PIERS Proceedings*, Guangzhou, China, Aug. 2014, pp. 2676–2680.

[25] K. P. Prokopidis and T. D. Tsiboukis, "Modeling of ground-penetrating radar for detecting buried objects in dispersive soils," *Appl. Comput. Electrom.*, vol. 22, pp. 287–294, 2007.

[26] K. P. Prokopidis and D. C. Zografopoulos, "Time-domain numerical scheme based on low-order partial-fraction models for the broadband study of frequency-dispersive liquid crystals," *J. Opt. Soc. Am. B*, vol. 33, no. 4, pp. 622–629, Apr 2016.

[27] S. J. Orfanidis, *Electromagnetic Waves and Antennas*. ECE Department Rutgers University, 2014. [Online]. Available: http://www.ece.rutgers.edu/∼orfanidi/ewa/

[28] J. A. Roden and S. D. Gedney, "Convolution PML (CPML): An efficient FDTD implementation of the CFS-PML for arbitrary media," *Microw. Opt. Techn. Let.*, vol. 27, pp. 334–339, 2000.

[29] K. Prokopidis and D. Zografopoulos, "Investigation of the stability of ADE-FDTD methods for modified Lorentz media," *IEEE Microw. Wireless Compon. Lett.*, vol. 24, no. 10, pp. 659–661, Oct 2014.